TISSUE ENGINEERING: Part A
Volume 19, Numbers 5 and 6, 2013
© Mary Ann Liebert, Inc.
DOI: 10.1089/ten.tea.2012.0047

Transplantation of Human Umbilical Cord Blood-Derived Mesenchymal Stem Cells or Their Conditioned Medium Prevents Bone Loss in Ovariectomized Nude Mice

Jee Hyun An, MD, PhD,[1] Hyojung Park, PhD,[1] Jung Ah Song, MS,[1] Kyung Ho Ki, MS,[1] Jae-Yeon Yang, PhD,[1] Hyung Jin Choi, MD,[1] Sun Wook Cho, MD, PhD,[1] Sang Wan Kim, MD, PhD,[1] Seong Yeon Kim, MD, PhD,[1] Jeong Joon Yoo, MD, PhD,[2] Wook-Young Baek, PhD,[3] Jung-Eun Kim, PhD,[3] Soo Jin Choi, MD, PhD,[4] Wonil Oh, MD, PhD,[4] and Chan Soo Shin, MD, PhD[1]

Umbilical cord blood (UCB) has recently been recognized as a new source of mesenchymal stem cells (MSCs) for use in stem cell therapy. We studied the effects of systemic injection of human UCB-MSCs and their conditioned medium (CM) on ovariectomy (OVX)-induced bone loss in nude mice. Ten-week-old female nude mice were divided into six groups: Sham-operated mice treated with vehicle (Sham-Vehicle), OVX mice subjected to UCB-MSCs (OVX-MSC), or human dermal fibroblast (OVX-DFB) transplantation, OVX mice treated with UCB-MSC CM (OVX-CM), zoledronate (OVX-Zol), or vehicle (OVX-Vehicle). Although the OVX-Vehicle group exhibited significantly less bone mineral density (BMD) gain compared with the Sham-Vehicle group, transplantation of hUCB-MSCs (OVX-MSC group) has effectively prevented OVX-induced bone mass attenuation. Notably, the OVX-CM group also showed BMD preservation comparable to the OVX-MSC group. In addition, microcomputed tomography analysis demonstrated improved trabecular parameters in both the OVX-MSC and OVX-CM groups compared to the OVX-Vehicle or OVX-DFB group. Histomorphometric analysis showed increased bone formation parameters, accompanied by increased serum procollagen type-I N-telopeptide levels in OVX-MSC and OVX-CM mice. However, cell-trafficking analysis failed to demonstrate engraftment of MSCs in bone tissue 48 h after cell infusion. *In vitro*, hUCB-MSC CM increased alkaline phosphatase (ALP) activity in human bone marrow-derived MSCs and mRNA expression of collagen type 1, *Runx2*, osterix, and *ALP* in C3H10T1/2 cells. Furthermore, hUCB-MSC CM significantly increased survival of osteocyte-like MLO-Y4 cells, while it inhibited osteoclastic differentiation. To summarize, transplantation of hUCB-MSCs could effectively prevent OVX-mediated bone loss in nude mice, which appears to be mediated by a paracrine mechanism rather than direct engraftment of the MSCs.

Introduction

Osteoporosis is characterized by the loss of bone mass and strength, which leads to fragility fractures, and has become a worldwide health problem among the elderly.[1] Most current therapies for osteoporosis, including bisphosphonates, estrogen, and selective estrogen receptor modulators, are antiresorptive agents that inhibit the bone-resorbing activity of osteoclasts.[2] Although these antiresorptive therapies have been shown to increase bone mineral density (BMD) and reduce the risk of fractures,[2] long-term safety and efficacy are ongoing concerns.[3,4]

Because osteoporosis results primarily from an imbalance between resorption and formation on endosteal and trabecular bone surfaces, anabolic therapy that directly stimulates bone formation by enhancing osteoblast activity is an another approach for treating osteoporosis. Teriparatide, the only currently available anabolic agent, effectively increases BMD and reduces the risk of fracture through new bone formation.[5,6] However, its use is limited due to its cost and the need for daily injection.

Stem cell therapy has emerged as a promising treatment modality for the repair and regeneration of damaged tissue in various conditions, including myocardial ischemia,[7,8] stroke,[9,10] diabetes,[11,12] and cartilage and bone defects,[13–15] owing to their multilineage differentiation potential. In this regard, systemic transplantation of mesenchymal stem cells (MSCs), which are precursors of osteoblasts, may be a reasonable approach for anabolic therapy for osteoporosis.

Departments of [1]Internal Medicine and [2]Orthopedics, Seoul National University College of Medicine, Seoul, Korea.
[3]Department of Molecular Medicine, Cell and Matrix Research Institute, Kyungpook National University School of Medicine, Daegu, Korea.
[4]Biomedical Research Institute, MEDIPOST, Co., Ltd., Seoul, Korea.

We previously reported the protective effect of systemic transplantation of syngeneic murine bone marrow-derived MSCs (BM-MSCs) that were retrovirally transduced with RANK-Fc[16] or RANK-Fc + CXCR4[17] in ovariectomy (OVX)-induced bone loss in mice. In these studies, transplantation of MSCs effectively prevents bone loss despite their poor BM homing and short-term engraftment, suggesting that these favorable effects are mediated by secretory factors from MSCs rather than direct engraftment. Several recent lines of evidence also support the hypothesis that therapeutic effects of stem cell transplantation are derived from secretory factors rather than by direct cell replacement. Indeed, a conditioned medium (CM) from MSCs has been shown to improve cardiac function after myocardial infarction,[18,19] accelerate wound healing,[20,21] and have neuroprotective effects.[22]

Although BM has been most commonly utilized as a source of MSCs, the number and multilineage differentiation capacity decline with the age or health condition of donors.[23–25] Moreover, obtaining BM is an invasive procedure that can cause complications such as pain, bleeding, and infection. To circumvent these limitations, umbilical cord blood (UCB) has been recently used as an alternative source of MSCs. UCB-derived MSCs (UCB-MSCs) have advantages over other sources of MSCs, including ease of harvesting and storage, less *in vitro* preaging, and low immunogenic potential.[26,27] Furthermore, UCB-MSCs may have a stronger capacity to differentiate into osteoblasts than other sources of MSCs,[28,29] indicating that UCB-MSCs may be a favorable potential source of stem cells for therapy for osteoporosis.

In our current study, we evaluated the effects of systemic injection of human UCB-MSCs (hUCB-MSCs) and their CM on OVX-induced bone loss in nude mice and investigated the mechanism of these effects *in vitro*.

Materials and Methods

Isolation and culture of hUCB-MSCs and preparation of CM

MSCs from hUCB were provided by MEDIPOST Co., Ltd. (Seoul, Korea). This study was approved by the Institutional Review Board of the Seoul National University Hospital and the Institutional Review Board of MEDIPOST Co., Ltd. The hUCB-MSCs were isolated and maintained as described.[30] From passage 4, MSCs were maintained in a MesenPRO RS™ basal medium (Gibco, Grand Island, NY) supplemented with MesenPRO RS Growth Supplement (Gibco) and 1% L-glutamine (Gibco). MSCs of passages 6–8 from one donor were used for all experiments.

The multilineage differentiation potential of the hUCB-MSCs was identified by culturing the cells in the presence of β-glycerophosphate (10 mM), dexamethasone (0.1 μM), and L-ascorbate 2-phosphate (50 μM) for osteogenic differentiation, by pellet culture in the presence of transforming growth factor-beta (TGF-β3; 10 ng/mL), 100 nM dexamethasone, 50 mg/mL insulin–transferrin–selenious acid + Premix (Becton Dickinson, Franklin Lakes, NY), 500 ng/mL bone morphogenic protein (BMP)-6 (R&D System, Minneapolis, MN), 100 μg/mL sodium pyruvate, 40 μg/mL L-proline, and 50 μg/mL L-ascorbate 2-phosphate (Sigma-Aldrich Corp., St. Louis, MO) for chondrogenic differentiation, and by culturing in the presence of dexamethasone (1 μM), 3-isobutyl-1-methylxanthine (0.5 mM), and insulin (10 μg/mL) for adipogenic differentiation. The cells were then stained with von Kossa, safranin O, and Oil Red O to observe osteogenic, chondrogenic, and adipogenic differentiation, respectively.

Human dermal fibroblasts (DFBs), isolated from foreskins of healthy donors aged 20–30 years (a kind gift from Dr. Jin Ho Chung, Seoul National University, Seoul, Korea), were cultured as described.[31] DFBs of passages 6–8 from one donor were used for all experiments.

Human BM-derived MSCs (hBM-MSCs) were obtained by aspiration from the iliac crest of subjects (23–78 years) undergoing hip prosthesis surgery due to non-necrotic hip disorders with ethics approval from the Seoul National University Hospital (Approval No. H-1101-108-353) using a modification of the procedure described by Pittenger *et al*.[32,33]

To prepare the CM from hUCB-MSCs, the cells were detached upon reaching 80% confluency in a 9-cm^2 dish and transferred into an α-minimum essential medium (MEM) containing 2% fetal bovine serum (FBS). After incubation for 24 h, the supernatant was collected and sterilized by the passage through a 0.45-μm-pore filter. We refer to the concentration of this medium as 1×.

Immunophenotypic analysis

To characterize cell surface expression of typical marker proteins, hUCB-MSCs were labeled with the following anti-human antibodies conjugated with FITC or phycoerythrin (PE): CD29-PE, CD44-PE, CD73-PE, CD90-PE, and CD166-PE; CD14-FITC, CD31-FITC, CD34-FITC, and CD45-FITC; HLA-ABC-FITC and HLA-DR-FITC (BD Biosciences, San Diego, CA); and CD105-PE (Serotec, Oxford, United Kingdom). Approximately 10,000 cells were measured using an FACScan flow cytometer (Becton Dickinson), and the results were analyzed with CellQuest software (Becton Dickinson). Similar results were obtained in three independent experiments.

Effects of hUCB-MSCs and CM on OVX nude mice

All animal experiments were reviewed and approved by the Institutional Animal Care and Use Committee of the Seoul National University (approval number: SNU-100311-1), and all animals were housed in the Centers for Laboratory Animal Care at the Seoul National University College of Medicine.

Experimental design. Female Balb/c nude mice aged 10 weeks were purchased from Orient Corporation (Kapyoung, Korea), and bilateral OVX or sham operation (Sham-op) was performed by standard methods under general anesthesia induced by subcutaneous injections of xylazine (2.2 mg/kg; Rompun; Bayer, Monheim, Germany) and tiletamine/zolazepam (6.0 mg/kg Zoletil 100; Virbac, Carros Cedex, France).[34] Four weeks after OVX or Sham-op (14 weeks old), the mice were divided into six groups as follows: (1) Sham-op mice injected with vehicle (Sham-Vehicle; $n = 8$), (2) OVX mice injected with vehicle (OVX-Vehicle; $n = 8$), (3) OVX mice injected with hUCB-MSCs (OVX-MSC; $n = 8$), (4) OVX mice injected with hUCB-MSC CM (OVX-CM; $n = 8$), (5) OVX mice injected with hDFBs (OVX-DFB; $n = 8$), and (6) OVX mice injected with zoledronate (OVX-Zol; $n = 8$).

On study days 1, 2, 8, and 9, 4×10^5 hUCB-MSCs in 100 μL of α-MEM (total of 16×10^5 cells, OVX-MSC group) or 100 μL of CM (total of 400 μL, OVX-CM group) was injected into the

lateral tail veins of mice. hDFBs were injected as a control, in the same manner as hUCB-MSCs to the OVX-DFB group. In the Sham-Vehicle and OVX-Vehicle groups, the culture medium (α-MEM) was injected each time. Zoledronate (100 μg/kg) was given subcutaneously at days 1 and 8 in the OVX-Zol group as a positive control.

Bone densitometry. Whole-body BMD and bone mineral content were measured at 4 weeks prior (before OVX or Sham-op) and 0 (before treatment), 4, and 8 weeks after treatment using a PIXImus II densitometer (software version 2.0; GE Lunar, Madison, WI) as described.[16]

Microcomputed tomography analysis. After 8 weeks of treatment, all mice were sacrificed, and right tibiae from each mouse were isolated and fixed in 70% ethanol for microcomputed tomography (microCT). MicroCT analysis of tibiae was obtained with a microCT scanner and software (model 1172; Skyscan, Antwerp, Belgium). Images were acquired at a voxel size of 9 μm, energy of 35 kV, and intensity of 220 μA. Two-dimensional images were used to generate 3D reconstructions using 3D Creator software supplied with the instrument.

Dynamic histomorphometric analysis. Mice were intraperitoneally injected with calcein (20 mg/kg body weight; Sigma-Aldrich Corp.) 2 and 7 days before sacrifice. The spine was isolated and fixed in 4% paraformaldehyde overnight at 4°C. Next, the undecalcified lumbar vertebrae were dehydrated in 70% ethanol followed by embedding in destabilized methylmethacrylate resin.[35] Five-micrometer-thick longitudinal serial sections were cut with an ultramicrotome, and the Bioquant program (Bio-Quant, Inc., San Diego, CA) was used for dynamic histomorphometric analysis.

Osteoclasts were enumerated on decalcified femora embedded in paraffin. Serial sections (6-μm thick) were prepared from paraffin blocks, stained for tartrate-resistant acid phosphatase (TRAP) activity, and counterstained with Alcian blue.

Biochemical markers of bone turnover. Blood samples were obtained through cardiac puncture at sacrifice, and sera were separated and stored at −70°C until analysis. Serum procollagen type-I N-terminal propeptide (P1NP) and TRAP were measured with mouse P1NP and TRAP enzyme-linked immunosorbent assay (ELISA) kits (IDS, Frankfurt, Germany), respectively, according to the manufacturer's instructions. Samples were measured at least in duplicate.

Cell trafficking analysis after transplantation of hUCB-MSCs

For *in vivo* cell trafficking analysis, a parallel experiment using fluorescent dye-labeled cell injection was performed. hUCB-MSCs were labeled with 3 μM carboxyfluorescein diacetate succinimidyl ester (CFDA SE) fluorescent dye (Vybrant CFDA SE Cell Tracer Kit; Invitrogen, Carlsbad, CA) according to the manufacturer's instructions for adherent cells. CFDA SE-labeled cells were counted, and viable cells were suspended in 100 μL culture medium (α-MEM) and injected into 14-week-old nude mice 4 weeks after OVX or Sham-op ($n=4$, each). Mice were sacrificed at 6, 24, 48, 72 h, and 1 week after CFDA SE-labeled cell injection, and the BM cells were analyzed for the presence of CFDA SE-positive cells (10^6 cells per sample) with FACSCalibur (Becton Dickinson) in the FL 1 channel (absorption at 495 nm and emission at 519 nm).[36] Cells isolated from mice that were injected with the α-MEM were used as a negative control, and positive controls were mice that received direct intrafemoral injection of CFDA SE-labeled cells.

Colony-forming unit assay

Female Balb/c nude mice aged 10 weeks underwent OVX or Sham-op followed by intravenous injection of hUCB-MSC CM or vehicle. The animals were sacrificed 7 days after injection, and BM cells were flushed from the femurs and tibiae of mice and plated in triplicate cultures (six-well plates) at a density of 1.0×10^6 cells/well with DMEM 4500 mg glucose/L, 10% FBS, 50 mM 2-mercaptoethanol, 100 mg/mL streptomycin, and 100 U/mL penicillin. The formation of colony-forming unit–fibroblasts (CFU-Fs) was evaluated after 14 days of culture in a humidified 5% CO_2/37°C environment. Cultures were washed with calcium- and magnesium-free Dulbecco's phosphate-buffered saline (PBS) twice and then fixed with cold ethanol. CFU-Fs were stained with Giemsa stain, and colonies with >50 cells counted using light microscopy. For colony-forming unit-osteoblast (CFU-OB), the cells were maintained in an osteogenic medium containing 10 mM β-glycerophosphate and 50 mg/mL of sodium 2-phosphate ascorbate. After 14 days, the cultures were terminated by washing with PBS twice and then fixed with cold ethanol. Formation of osteoblast progenitors was detected using an alkaline phosphatase (ALP) reagent (86-R; Sigma-Aldrich Corp.), and ALP-positive colonies were counted.[37]

In vitro *effect of hUCB-MSC CM on ALP activities*

The effect of hUCB-MSC CM on osteogenic differentiation was analyzed using C3H10T1/2 cells, a murine embryonic mesenchymal cell line, and hBM-MSCs. C3H10T1/2 cells or hBM-MSCs were seeded into 24-well plates at 50,000 cells/well and grown to 90% confluence within 2 days. Osteogenic differentiation was induced with β-glycerophosphate (10 mM) and L-ascorbic acid (50 μM) in the presence or absence of 1× or 0.5× hUCB-MSC CM. After 7 days of osteogenic induction, ALP activities were measured as described.[38]

Transient transfection and luciferase assay

The TOPflash reporter construct was kindly provided by Dr. Roberto Civitelli (Washington University, St. Louis, MO). BRE-Luc, a BMP-responsive reporter, was from Dr. Jung Tae Koh (Chonnam National University, Kwangju, Korea). −1.3OG2-Luc, a 1.3-kb murine osteocalcin (*OC*) promoter that contains one binding site for Runx2, was a kind gift from Dr. Patricia Ducy (Columbia University, New York, NY). p3TP-Lux, which contains a TGF-β-response element, was purchased from Addgene (Cambridge, MA). C3H10T1/2 cells were seeded into 24-well plates at 1.5×10^4 cells/well, and 12 h later, reporter vectors were transiently transfected into the cells. Twenty-four hours after transfection, the cells were treated with hUCB-MSC CM or the control medium for 24 h. As a positive control, Wnt-3A CM (0.5×), BMP-2

(100 ng/mL), or TGF-β (5 nM) was added to cells transfected with TOPflash, BRE-Luc, or p3TP-Lux, respectively. For the −1.3OG2-Luc reporter, 400 ng/well pcDNA3-HA-til (a kind gift from Dr. Je-Yong Choi, Kyungpook National University, Deagu, Korea), an expression vector for the type 2 Runx2 isoform, was cotransfected. Cell lysates were collected using the Dual luciferase assay system (Promega, Madison, WI), and luciferase activity was measured with a luminometer (Lumat LB 9507, Berthold, Germany). As the internal standard, pRL-TK *Renilla* luciferase control vector (Promega) was also cotransfected to normalize for transfection efficiency. All luciferase activity values were normalized to *Renilla* luciferase activity and expressed as the fold induction relative to the basal promoter activity.

Quantitative real-time reverse transcription–polymerase chain reaction measurements of gene expression

mRNA expression of osteoblast-specific genes (*Runx2*, *OC*, osterix, collagen type 1 [*Col1*], and *ALP*) was determined with quantitative real-time reverse transcription–polymerase chain reaction (RT-PCR). cDNA was synthesized with 1 μg total RNA using a Reverse Transcription System kit (Promega). Quantitative PCR was performed with the real-time SYBR Green PCR method using the ABI PRISM 7900 HT sequence detection system (Applied Biosystems, Carlsbad, CA). The primers used are listed in Supplementary Table S1 (Supplementary Data are available online at www.liebertpub.com/tea). Amplification was performed in a 20-μL volume, using 2× Universal SYBR PCR Master Mix (PerkinElmer, Covina, CA). Thermal cycling conditions were as follows: 10 s at 95°C, 40 cycles of 30 s at 95°C, 30 s at 52°C, and 30 s at 72°C. Relative gene expression was calculated by comparing the cycle threshold (C_T) ratios to that of the reference gene, β-actin. All PCRs were performed at least in duplicate.

In vitro *effect of hUCB-MSC CM on osteoclastic differentiation*

To evaluate the effect of hUCB-MSC CM on osteoclastic differentiation, bone marrow macrophages (BMMs) were isolated from 6-week-old C57BL/6 male mice as described.[39] Briefly, total BM cells from femora and tibiae were flushed out using a 27-gauge needle, and the resulting cells were cultured in an α-MEM supplemented with 10% FBS, 1% glutamine, and 30 ng/mL macrophage colony-stimulating factor (M-CSF) for 3 days. To induce osteoclast formation, BMMs were treated with M-CSF (30 ng/mL) and receptor activator of nuclear factor kappa-B ligand (RANKL; 50 ng/mL) in the presence or absence of 0.5× or 1× hUCB-MSC CM in 96-well culture plates (Corning LifeSciences, Edison, NJ). Cells were fixed and stained for TRAP according to the manufacturer's instructions (Sigma-Aldrich Corp.).

In vitro *effect of hUCB-MSC CM on osteocyte morphology and survival*

The osteocyte-like cell line, MLO-Y4, was kindly provided by Dr. Linda Bonewald (University of Missouri-Kansas City). To examine the ultrastructural changes of MLO-Y4 cells, the cells were visualized with electron microscopy after fixation with 2.5% glutaraldehyde in 0.1 M phosphate buffer (pH 7.4), followed by processing for transmission and scanning electron microscopy (TEM and SEM), as described.[38] To measure the dendrite length, number of mitochondria, and autophagosome to cytoplasmic area, 10 randomly selected fields per condition were examined with the point counting method by two independent examiners (J.A.S. and J.Y.Y.) blinded to the design.

Osteocyte viability was determined using an MTT [3-(4, 5-dimethylthiazol-2-yl)-2,5-diphenyltetrazolium bromide] assay. MTT was dissolved in PBS (0.5 mg/mL) and sterilized by passage through a 0.22-μm filter. To induce apoptosis, MLO-Y4 cells were treated with 10^{-6} M dexamethasone in the presence or absence of hUBC-MSC CM for 24 h. After 24 h, 30 μL MTT stock solution was added to each well. After incubation for 4 h at 37°C, 30 μL dimethyl sulfoxide was added to all wells after removing the MTT solution, and mixed thoroughly to lyse the cells and dissolve the dark blue crystals. After 5 min, the absorbance was read with an ELISA reader (ThermoMax; Scientific Surplus, Hillsborough, NJ) at a wavelength of 540 nm.

Statistical analysis

Statistical significance was analyzed with the nonparametric Mann–Whitney test or Wilcoxon matched-pair test for group comparison, and $p < 0.05$ was considered significant. Data are shown as the means ± standard deviation (SD) or standard error of the mean. SPSS software (version 16.0, SPSS Inc., Chicago, IL) was used for statistical analyses.

Results

Characterization of hUCB-MSCs

hUCB-MSCs were analyzed by flow cytometry to detect surface antigens. The hUCB-MSCs were positive for CD29 (β1-integrin), CD44 (hyaluronate receptor), CD73, CD90, CD105, CD166, and HLA-ABC. This immunophenotype was very similar to that of BM-derived MSCs. Markers of the hematopoietic lineage, including CD14, CD31, CD34, CD45, and HLA-DR, were not expressed (data not shown). The multilineage differentiation potential of hUCB-MSCs was confirmed under specific culture conditions for induction of the respective cell types. The cells showed high osteogenic and chondrogenic differentiation potential, whereas the capacity to differentiate into adipocytes was relatively limited (Supplementary Fig. S1).

Systemic injection of hUCB-MSCs or CM reduces OVX-induced bone mass attenuation in nude mice

Whole-body BMD measurement with Piximus showed that OVX groups (OVX-Vehicle, OVX-MSC, OVX-CM, and OVX-Zol groups together, $n = 32$) exhibited significantly less BMD gain compared to the Sham-Vehicle group ($n = 8$; +4.5% ± 0.8% vs. +7.3% ± 0.9%, $p < 0.001$) after OVX, as expected (Fig. 1A). Of note, mice at this age are still growing, and all animals actually gained bone mass during the study period. Transplantation of hUCB-MSCs into OVX mice (OVX-MSC group) at this point prevented OVX-induced bone mass attenuation, so that the percent increase of BMD relative to baseline in the OVX-MSC group was significantly greater compared with the OVX-Vehicle group (8.4% ± 0.7%

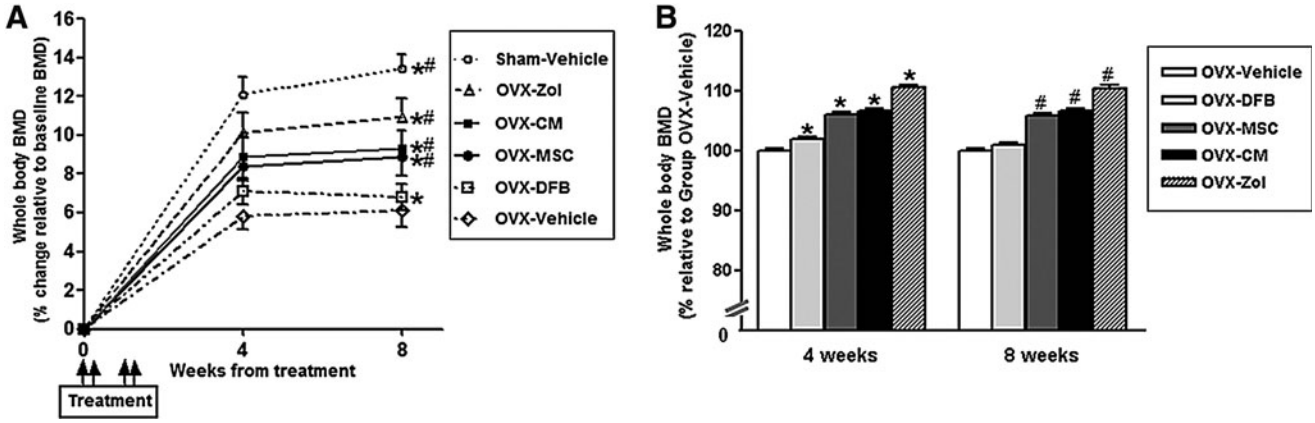

FIG. 1. Bone mineral density (BMD) changes in the animals. Percent changes of BMD relative to baseline of each group **(A)** and BMD relative to the ovariectomy (OVX)-Vehicle group **(B)**. Ten-week-old female nude mice were sham-operated (Sham-op) or OVX and randomized into six groups; Sham-op + Vehicle mice ($n = 8$), OVX + Zoledronate (Zol) mice ($n = 8$), OVX + human umbilical cord blood mesenchymal stem cell (hUCB-MSC)-conditioned medium (OVX + CM) mice ($n = 8$), OVX + hUCB-MSCs ($n = 8$), OVX + human dermal fibroblast (hDFB) (OVX + DFB), or OVX + Vehicle mice ($n = 8$). The mice were injected with vehicle, hUCB-MSC CM, hUCB-MSCs, or hDFBs at days 1, 2, 8, and 9, and BMD (g/cm^2) was measured with a PIXImus densitometer at 4-week intervals as indicated. For the OVX-Zol group, zoledronate (100 μg/kg) was given at days 1 and 8. Data are the means ± standard deviation (SD). $^*p < 0.01$ versus OVX-Vehicle at 4 weeks, $^{\#}p < 0.01$ versus OVX-Vehicle at 8 weeks.

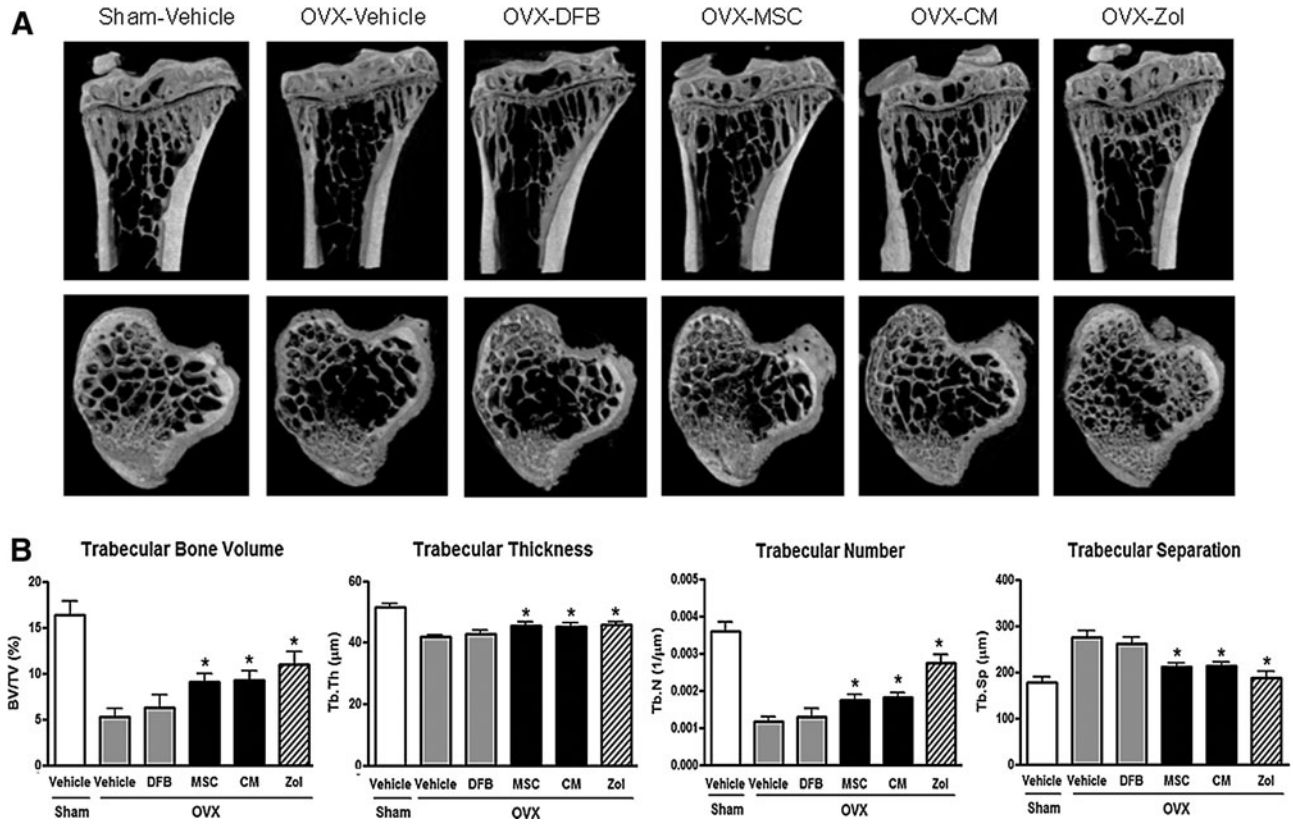

FIG. 2. Bone microstructure changes in the animals. Tibiae of the nude mice were removed and evaluated *ex vivo* by microcomputed tomography (microCT) 8 weeks after treatment as in **(A)**. **(A)** Representative microCT images of the tibiae. **(B)** Quantitative changes in trabecular parameters, including trabecular bone volume expressed as percentage of total tissue volume (BV/TV), trabecular thickness (Tb.Th), trabecular number (Tb.N), and trabecular separation (Tb.Sp). $^*p < 0.05$ versus OVX-Vehicle. Data are the means ± SD.

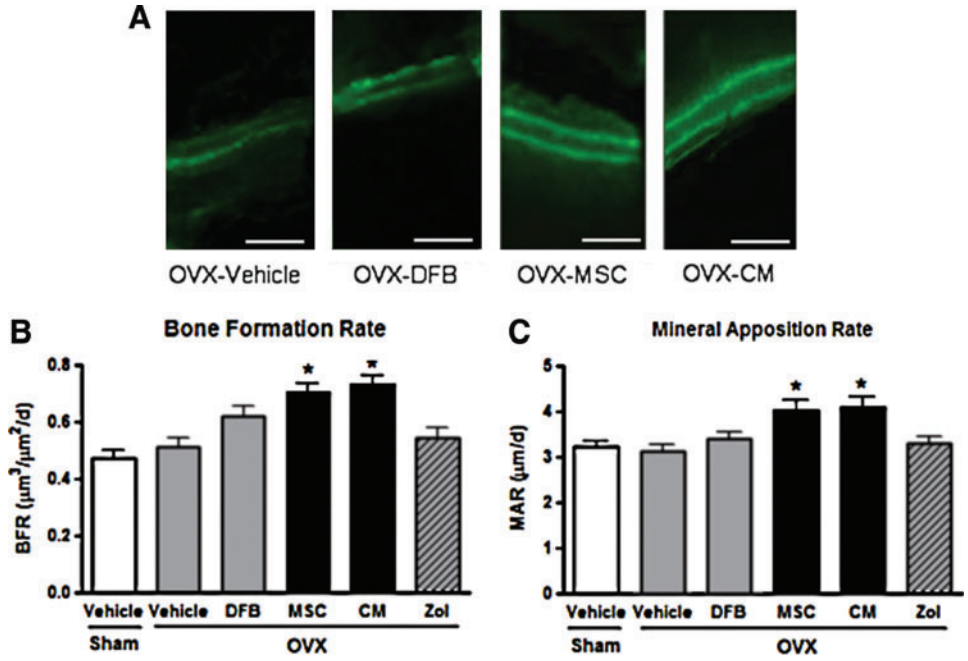

FIG. 3. Dynamic histomorphometric analysis of the spine in the animals. **(A)** Representative fluorescent images obtained from lumbar spine after calcein double labeling. Scale bar = 100 μm. Dynamic histomorphometric measurements, including bone formation rate **(B)** and mineral apposition rate **(C)**, were obtained from the lumbar spine using Bio-Quant software. Data are the means ± SD. *$p < 0.05$ versus OVX-Vehicle. Color images available online at www.liebertpub.com/tea

vs. 5.8% ± 0.7% at 4 weeks, $p < 0.01$; 8.9% ± 1.0% vs. 6.1% ± 0.9% at 8 weeks, $p < 0.01$; Fig. 1A). The BMD gain in the OVX-MSC group was ~80% of that in the OVX-Zol group. Transplantation of hDFBs into OVX mice (OVX-DFB group) also slightly prevented OVX-induced bone mass attenuation at 4 weeks; however, it was not maintained to 8 weeks. Notably, treatment with CM alone also significantly prevented OVX-induced BMD attenuation (8.9 ± 0.7 at 4 weeks, 9.3 ± 1.0 at 8 weeks, both $p < 0.01$ compared with the OVX-Vehicle group), which was comparable to that observed in the OVX-MSC group. Figure 1B showed relative BMD of each group compared with the OVX-vehicle group. Consistent with BMD results, *ex vivo* microCT analysis of proximal tibiae at 8 weeks after treatment demonstrated a significant increase in trabecular bone volume, trabecular thickness, and trabecular number in both the OVX-MSC and OVX-CM groups compared with the OVX-Vehicle group or OVX-DFB group, whereas trabecular separation was reciprocally reduced (Fig. 2A, B). The cortical phenotype measured in the mid-diaphysis of tibiae showed no significant difference between the OVX-MSC or OVX-CM group compared with the OVX-Vehicle group (Supplementary Table S2). Transplantation of hDFBs into OVX mice (OVX-DFB group) did not significantly affect either trabecular or cortical parameters (Fig. 2A and B and Supplementary Table S2).

Dynamic histomorphometric analysis with calcein double labeling of the lumbar spine also revealed significant increases in the bone formation rate and mineral apposition rate in the OVX-MSC and OVX-CM groups compared with the OVX-Vehicle group (Fig. 3). Furthermore, consistent with these histomorphometric parameters, serum levels of P1NP, a marker of bone formation and osteoblastic activity, were significantly higher in the OVX-MSC and OVX-CM groups compared with the OVX-Vehicle group at 8 weeks (Fig. 4A). However, osteoclast numbers, bone resorption surface (data not shown), and serum TRAP levels (Fig. 4B) were not significantly different between the OVX-Vehicle group and the OVX-MSC or OVX-CM groups, suggesting that treatment with MSCs and CM did not affect bone resorption or osteoclastic activities.

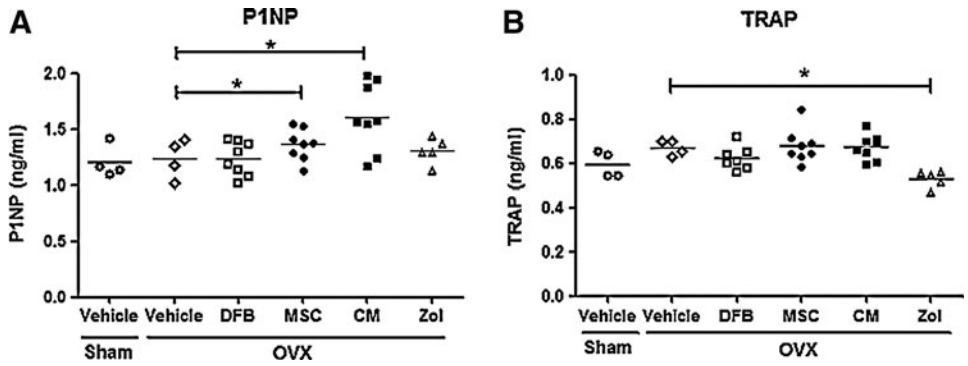

FIG. 4. Serum levels of biochemical markers of bone turnover. Serum levels of procollagen type-I N-terminal propeptide (P1NP), a bone formation marker **(A)**, and TRAP5b, a bone resorption marker **(B)**, 8 weeks after treatment as in Fig. 2. Data are the means ± SD. *$p < 0.05$ versus OVX-Vehicle.

Table 1. Fluorescence-Activated Cell-Sorting Analysis of Carboxyfluorescein Diacetate Succinimidyl Ester-Labeled Umbilical Cord Blood Mesenchymal Stem Cells from Bone Marrow

	0 h	*6 h*	*24 h*	*48 h*	*72 h*	*1 week*
Sham-Vehicle($n=4$)	0.10 ± 0.03	0.09 ± 0.04	0.12 ± 0.03	0.10 ± 0.04	0.09 ± 0.03	0.11 ± 0.04
OVX-Vehicle($n=4$)	0.11 ± 0.02	0.12 ± 0.03	0.10 ± 0.04	0.13 ± 0.05	0.11 ± 0.03	0.10 ± 0.04
OVX-MSC($n=4$)	0.12 ± 0.03	1.05 ± 0.10[a]	0.62 ± 0.11[a]	0.16 ± 0.07	0.12 ± 0.04	0.11 ± 0.03
OVX-DFB($n=4$)	0.10 ± 0.02	0.34 ± 0.08[a]	0.16 ± 0.03	0.13 ± 0.04	0.11 ± 0.04	0.10 ± 0.02
OVX-Direct injection($n=4$)	0.11 ± 0.04	27.01 ± 2.45[a]	19.90 ± 3.41[a]	7.06 ± 1.61[a]	3.13 ± 1.13[a]	0.73 ± 0.11[a]

Values are forward scatter intensity value.
[a]$p<0.01$ versus 0h.
DFB, dermal fibroblast; MSC, mesenchymal stem cell; OVX, ovariectomy.

Short-term trafficking of hUCB-MSCs after systemic transplantation

To investigate whether the bone-protective effect of hUCB-MSCs was due to homing and direct engraftment of the cells into BM, CFDA SE-labeled MSCs were injected to OVX mice, and BM cells were analyzed by FACS at 6, 24, 48, 72 h, and 1 week after injection as a parallel experiment. However, as shown in Table 1, the fraction of CFDA SE-positive cells in BM of the OVX-MSC group was only 1.05% ± 0.09% at 6 h after cell transplantation, and it gradually decreased over time so that no CFDA SE-labeled cells were observed after 48 h.

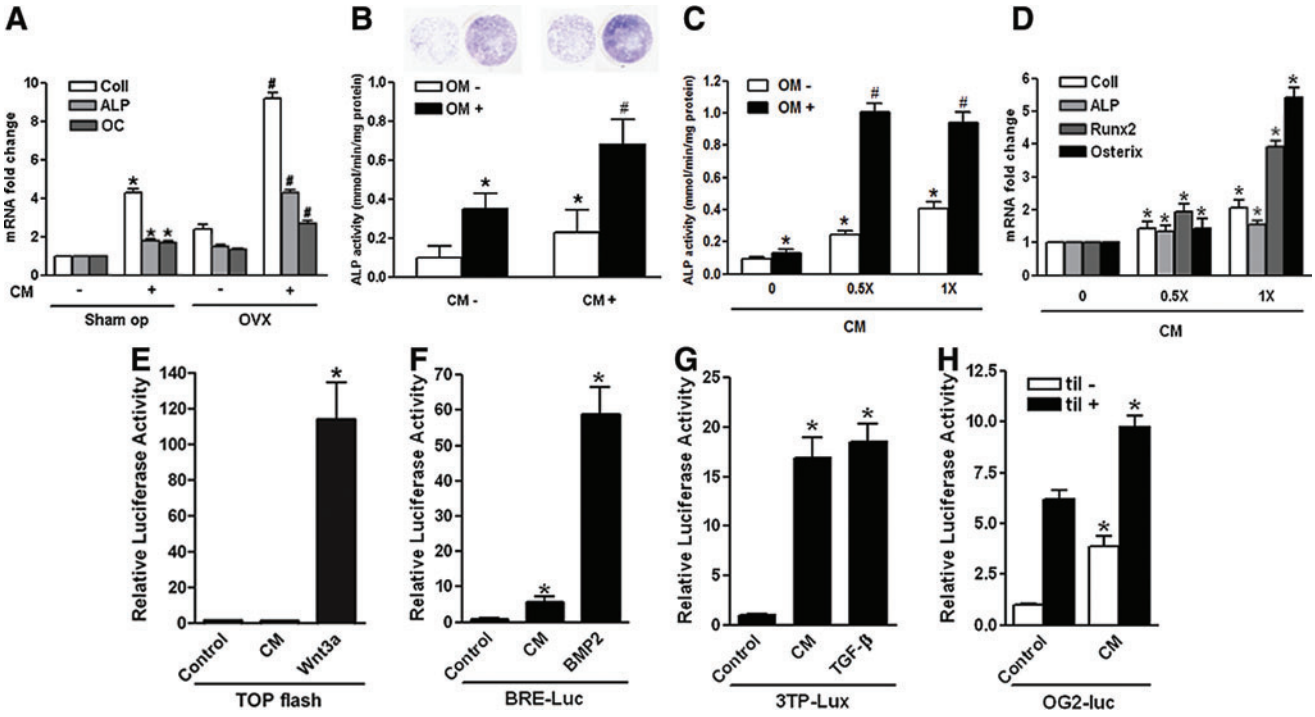

FIG. 5. Effects of hUCB-MSC CM on osteoblastic differentiation *in vivo* and *in vitro*. **(A)** Human UCB-MSC CM or vehicle was injected to 10-week-old female nude mice after Sham-op or OVX. After 7 days, femora and tibiae were harvested, and mRNA for osteoblast products was determined by real-time quantitative polymerase chain reaction (PCR). Data are the means ± SD. *$p<0.01$ versus Sham-op CM (−); #$p<0.01$ versus OVX CM (−). **(B, C)** Human bone marrow-derived MSCs or C3H10T1/2 cells were cultured, and osteogenic differentiation was induced with an osteogenic medium (OM) containing β-glycerophosphate (10 mM) and L-ascorbic acid (50 μM) in the presence or absence of hUCB-MSC CM. Alkaline phosphatase (ALP) activities were measured after 7 days. Data are the means ± SD. *$p<0.01$ versus OM - CM 0; #$p<0.01$ versus OM + CM 0. **(D)** Total RNA was extracted from C3H10T1/2 cells grown for 5 days in the presence or absence of 0.5× or 1× hUCB-MSC CM. The amount of mRNA for osteoblast products was determined by real-time quantitative PCR and expressed as the mRNA abundance relative to vehicle treatment. Data are the means ± SD. *$p<0.01$ versus CM 0. **(E–H)** C310T1/2 cells were transiently transfected with TOPflash, BRE-Luc, p3TP-Lux, or −1.3OG2-Luc. Cells were then exposed to either vehicle or hUCB-MSC CM (1×). Wnt-3A CM, bone morphogenic protein (BMP)-2, or transforming growth factor (TGF)-β was added as a positive control for TOPflash, BRE-Luc, or p3TP-Lux, respectively. For −1.3OG2-Luc, expression vector for til (pcDNA3-til) was cotransfected as a positive control. Forty-eight hours after transfection, the cells were harvested and used for luminometry. Luciferase activities were normalized for transfection efficiency using *Renilla* activity, and all values were expressed as the fold induction relative to basal promoter activity. Data are the means ± SD, and the graphical results are representative of three independent experiments, each performed in triplicate. *$p<0.01$ versus control. Color images available online at www.liebertpub.com/tea

Effect of CM on bone cells in vivo *and* in vitro

Because transplanted hUCB-MSCs did not show long-term engraftment in BM, and the protective effect of CM from hUCB-MSCs was comparable to that of transplantation of hUCB-MSCs *per se*, we postulated that the therapeutic effect of hUCB-MSCs may originate from secretory factors from MSCs. We therefore evaluated the effect of CM on bone cells *in vivo* and *in vitro*. First, we investigated the effects of hUCB-MSC CM on the BM stem cell population *in vivo* using female Balb/c nude mice that underwent OVX or Sham-op, followed by intravenous injection of hUCB-MSC CM or vehicle. However, we were unable to document any significant difference in the number of CFU-Fs and CFU-OB between mice injected with hUCB-MSC CM and those treated with vehicle regardless of the OVX state (data not shown). In contrast, when we analyzed the mRNA expression of osteoblast-specific genes from bone, the mRNA levels of *Col1*, *ALP*, and *OC* were significantly increased in mice injected with hUCB-MSC CM compared with those treated with vehicle (Fig. 5A).

We then studied the effect of hUCB-MSC CM on osteoblastic differentiation *in vitro*. As shown in Figure 5B, culturing human BM-derived MSCs in osteogenic medium for 7 days resulted in induction of osteoblastic differentiation as measured by increased ALP stain and activities. Treatment with hUCB-MSC CM (0.5×) in this context has significantly increased ALP activity by approximately twofold compared to vehicle treatment (Fig. 5B). Interestingly, treatment with CM alone also enhanced ALP activity, up to 1.5-fold, even in the absence of an osteogenic medium.

Similarly, treatment of the mouse embryonic mesenchymal cell line C3H10T1/2 with hUCB-MSC CM has resulted in a significant increase in ALP activities in a dose-dependent manner (Fig. 5C). Furthermore, mRNA expression of the osteoblast-specific genes, including *Col1*, *ALP*, *Runx2*, and

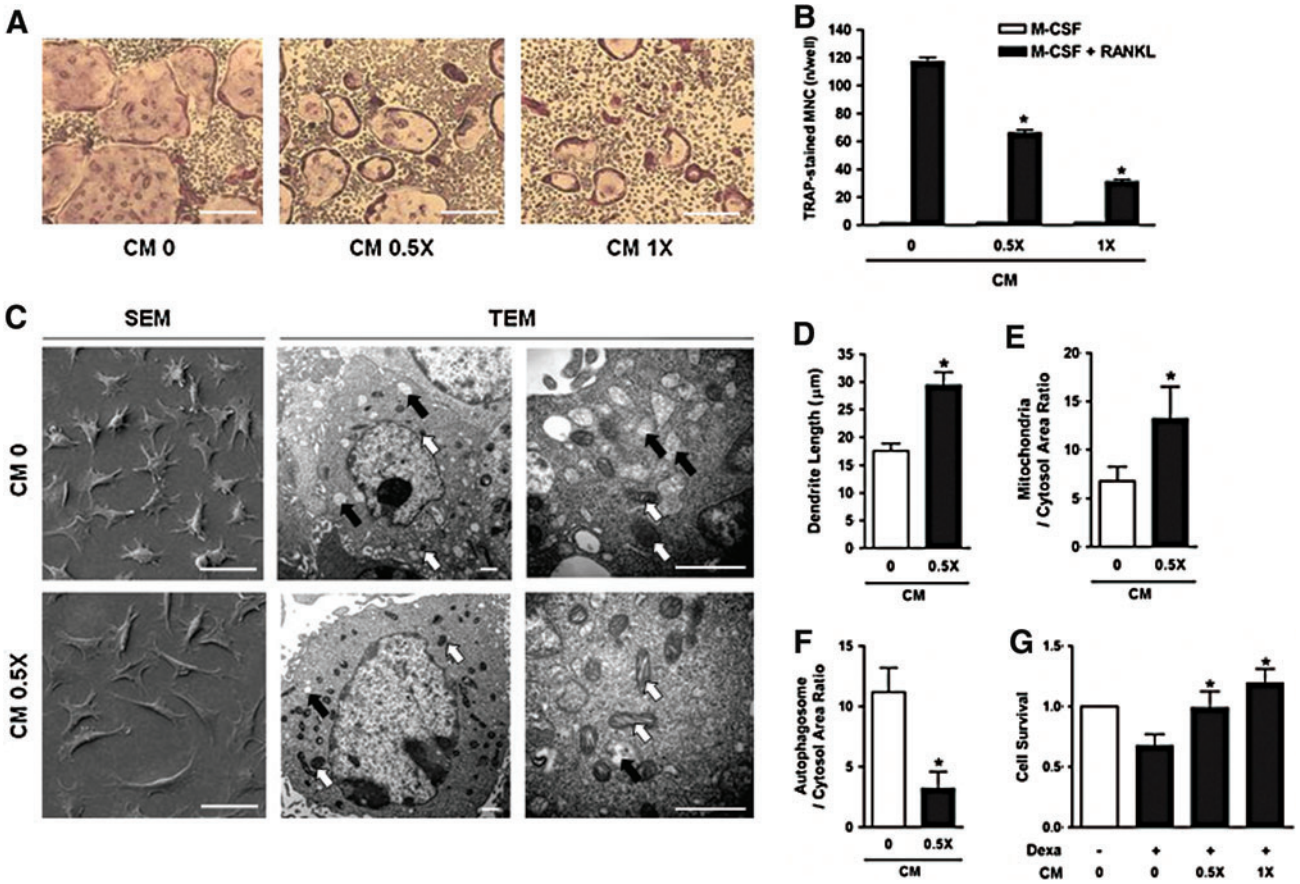

FIG. 6. Effects of UBC-MSC CM on osteoclastogenesis and MLO-Y4 cells *in vitro*. Bone marrow macrophages (BMMs) were isolated from C57BL/6 mice and cultured with macrophage colony-stimulating factor (M-CSF) and receptor activator of nuclear factor kappa-B ligand (RANKL) in the absence (CM 0) or presence of hUCB-MSC CM (CM 0.5× and CM 1×). Representative tartrate-resistant acid phosphatase (TRAP)-stained osteoclasts (scale bars, 100 μm) **(A)** and the number of TRAP-positive multinucleated cells isolated $*p < 0.01$ versus CM 0. **(B)**. **(C)** MLO-Y4 cells were observed with a scanning or transmission electron microscope (SEM or TEM) after treatment with vehicle (CM 0) or 0.5×hUCB-MSC CM (CM 0.5×) for 72 h. Scale bars, SEM = 50 μm, TEM = 1 μm. Average lengths of dendrite **(D)**, ratio of mitochondria (white arrow) to cytosol area **(E)**, and ratio of autophagosome (black arrow) to cytosol area **(F)** were calculated. $*p < 0.01$ versus CM 0. To investigate the effects of CM on cellular apoptosis of MLO-Y4 cells, the cells (2×10^3 cells/well) were plated and cultured for 24 h in the presence or absence of dexamethasone and/or hUCB-MSC CM (0.5× or 1×) as indicated. Cell viability was quantified with the MTT calorimetric assay. Data are the means ± SD, and the graphical results are representative of three independent experiments, each performed in triplicate. $*p < 0.01$ versus Dexa + CM 0 **(G)**. Color images available online at www.liebertpub.com/tea

osterix, was also significantly increased by treatment with CM in a dose-dependent manner (Fig. 5D).

We next studied which of the signaling pathways was activated to enhance osteoblastic differentiation of the mesenchymal cells after treatment with the CM. We performed promoter reporter assays that evaluate the activities of the Wnt, BMP-2, Runx2, and TGF-β pathways by transient transfection of the TOPflash, BRE-Luc, −1.3OG2-Luc, and p3TP-Lux reporter plasmids into C3H10T1/2 cells, respectively. As shown in Figure 5E, treatment of C3H10T1/2 cells with hUCB-MSC CM did not activate TOPflash activity, whereas Wnt-3A CM has robustly upregulated it. However, hUCB-MSC CM significantly increased BRE-Luc (Fig. 5F) and p3TP-Lux (Fig. 5G) activity by 5.7-fold and 16.9-fold, respectively. The luciferase activity from p3TP-Lux was ~90% of that induced with 5 nM TGF-β. In addition, the CM significantly increased the −1.3OG2-Luc reporter activity by fourfold and further enhanced til-mediated activity by 60% (Fig. 5H).

Next, we evaluated the effects of the CM on osteoclastic differentiation using BMMs isolated from C57Bl/6 mice. When the cells were cultured in the presence of M-CSF and RANKL to induce osteoclastic differentiation, addition of hUCB-MSC CM significantly reduced the number of TRAP-positive multinucleated cells in a dose-dependent manner 4–5 days after culture (Fig. 6A, B).

Finally, we examined the effects of CM on cell morphology and survival of MLO-Y4 cells, which exhibit characteristics of osteocytes. SEM examination showed that treatment of MLO-Y4 cells with CM for 48 h enhanced the extension of dendritic processes, while the proportion of the cytoplasm was reciprocally decreased (Fig. 6C SEM and D). We also observed increased numbers of mitochondria (Fig. 6C TEM and E) and decreased numbers of autophagosomes (Fig. 6C TEM and F) in CM-treated MLO-Y4 cells by TEM examination. Moreover, when cellular apoptosis was induced with dexamethasone, treatment with the CM significantly enhanced cell survival in a dose-dependent manner (Fig. 6G).

Taken together, these results suggest that secretory factors from hUCB-MSCs enhanced osteoblastic differentiation, osteocyte-like morphological changes, and survival of osteocytes, and inhibited osteoclastic differentiation.

Discussion

In our current study, we demonstrated for the first time that systemic transplantation of hUCB-MSCs, which have advantages over other sources of MSCs, prevented OVX-induced bone loss in nude mice. Because transplanted hUCB-MSCs did not show long-term engraftment to BM over 48 h, and the protective effects of hUCB-MSC CM were comparable to transplantation of hUCB-MSCs *per se*, we postulated that the therapeutic effects of hUCB-MSCs on bone were derived from secretory factors from MSCs rather than by direct engraftment of cells. This hypothesis was supported by the *in vitro* assays in which the CM enhanced osteoblastic differentiation and osteocyte survival and inhibited osteoclastic differentiation.

Although MSCs isolated from BM have been the mainstay for use in stem cell therapy, hUCB-MSCs have unique advantages over BM-MSCs. In addition to the relative ease of harvesting and storage, hUCB-MSCs do not actively provoke proliferation and suppress the allogeneic proliferation of responder lymphocytes, indicating their usefulness in allogeneic cell therapies.[40]

In this study, we found that transplantation of hUCB-MSCs resulted in clear reversal of the negative impacts of OVX on bone mass. First, mice injected with hUCB-MSCs gained an average of ~30% more BMD compared to mice treated with vehicle at 4 and 8 weeks after OVX. Second, trabecular volume, trabecular number, and trabecular thickness were all increased, whereas the trabecular separation was significantly decreased. Third, dynamic histomorphometric analysis showed a decreased rate of bone formation with a concomitant increase in serum P1NP levels after transplantation of hUCB-MSCs, whereas the TRAP level was not significantly changed. These results indicate that the beneficial effects of hUCB-MSC transplantation result from anabolic effects on trabecular bone. These results are in good agreement with our recent study that demonstrated anabolic effects of transplantation of human adipocyte-derived MSCs in nude mice after OVX.[41]

The major problem in treating osteoporosis with systemic transplantation of MSCs is their poor BM homing and engraftment efficiencies. Indeed, our previous study that evaluated the effects of syngeneic transplantation of BM-MSCs with retroviral transduction of RANK-Fc, a soluble inhibitor of osteoclast differentiation, demonstrated poor homing of transplanted cells to bone tissue *in vivo*.[16] Furthermore, cotransduction of CXCR4, a chemokine that enhances homing to BM spaces across the stromal cell-derived factor-1 gradient, did not improve engrafting of the transplanted BM-MSCs in the long term, although the bone mass gain was greater compared with that achieved by CXCR4 (−) cells.[17] Consistent with these studies, the efficiencies of short-term homing and long-term engraftment of hUCB-MSCs in this study do not seem to be sufficient for any positive effects on bone mass. Using adipocyte-derived MSC transplantation, we found that most transplanted cells are trapped in the lung 48 h after intravenous injection.[41] Cell trafficking analysis of PKH26 fluorescence demonstrated transient appearance of the injected cells, mostly in the liver, heart, and spleen. Although a low signal is also detected in bone tissues, the signal disappears 72 h after injection, indicating that virtually no cells become engrafted over the long term.[41] From these results, the effects of hUCB-MSC cell therapy we observed in this study may also be due to paracrine or trophic effects of the stem cells maybe from other tissues rather than direct engraftment of the injected cells to BM. In support of this notion, we observed that injection of CM from hUCB-MSCs also resulted in significant protection against OVX-induced bone loss in these animals. The effect of CM injection was comparable to that achieved by hUCB-MSC injection. Our result is analogous to a previous study, which evaluated the effects of CM *in vitro* or *ex vivo*. Indeed, a recent study by Walter *et al*. showed that MSC CM significantly enhances wound closure rates, whereas CM from L929 or HaCaT cultures does not, an effect that seems to be a consequence of accelerated cell migration.[21] In addition, MSC-derived CM promotes proliferation of cardiac progenitor cells and inhibits apoptosis induced by hypoxia and serum starvation.[42] More recently, Jung *et al.* showed that *ex vivo* culture of MSCs in the presence of human cord blood serum results in selective activation of platelet-derived

growth factor and epidermal growth factor signals in MSCs, and that the cells exhibit higher self-renewal and enhanced osteogenic potential.[43] All of these studies demonstrated the beneficial effects of MSC CM or cord blood serum in terms of cell proliferation or local tissue repair. Now, with the addition of our new study, it appears that systemic administration of hUCB-MSC CM also contributes to bone mass sparing in the OVX model *in vivo*.

We found that injection of hUCB-MSC CM to nude mice did not significantly increase the number of CFU-Fs or CFU-OB. However, the mRNA expression of *Col1*, *ALP*, and *OC* in bone tissues, the markers of osteoblast differentiation, was significantly increased by CM injection. These results suggest that injection of hUCB-MSC CM does not drive the lineage allocation of BM stem cells, but activates the cells already committed to the osteoblastic lineage. *In vitro*, hUCB-MSC CM also significantly enhanced ALP activities and osteoblast-specific gene expression compared with vehicle treatment, suggesting that hUCB-MSC CM has pro-osteogenic properties. Furthermore, hUCB-MSC CM significantly upregulated major signaling pathways involved in osteoblast differentiation, including the BMP-2, TGF-β, and Runx2 pathways. Although we have not identified the specific molecules that induce these signaling pathways, our results suggest that hUCB-MSC CM contains a number of factors that may cooperatively enhance osteoblastic differentiation through multiple mechanisms. In support of our notion, Jung *et al.* recently demonstrated that MSCs cultivated in cord blood serum exhibit enhanced basal and Runx2-mediated transcriptional activation of the *OC* promoter with preferential differentiation into osteogenic lineages, whereas adipogenic differentiation is suppressed.[43]

Using an *in vitro* BMM culture study, we found that osteoclast differentiation from BMMs was also significantly suppressed by treatment with hUCB-MSC CM, suggesting that hUCB-MSC CM has both pro-osteogenic and anti-osteoclastogenic potential. However, inhibition of osteoclast formation is not consistent with the absence of bone resorption parameter changes, including osteoclast number, bone resorption surface, and serum levels of TRAP in mice that received hUCB-MSC CM. Although the reason for this apparent discrepancy is not clear, we speculate that unlike *in vitro* BMM culture conditions, increased osteoblast differentiation by hUCB-MSC CM may have contributed to osteoclast formation, perhaps through the RANKL-RANK system, thereby offsetting the suppressive effects on osteoclast formation we observed *in vitro*.

Importantly, we also identified beneficial effects of hUCB-MSC CM on osteocyte survival and activity. Osteocytes were recently recognized as critical elements in the physiological status of the bone microenvironment.[44] The differentiation of osteoblasts into osteocytes during bone formation is accompanied by a 70% reduction in cell body volume due to the redistribution of the cytoplasm to dendritic processes, leading to dendritic enlongation.[45] Therefore, in conjunction with increased numbers of mitochondria and decreased numbers of autophagosomes, the enhanced dendrite formation we observed in this study indicates that treatment with CM resulted in enhanced survival and function of osteocytes. Furthermore, treatment with CM mitigated the cell death induced by dexamethasone. Because osteocyte cell death can occur in association with pathologic conditions such as osteoporosis and osteoarthritis, leading to increased skeletal fragility,[46–48] these results suggest that hUCB-MSC CM may contribute to bone mass preservation in osteoporosis models. Taken together, our data indicate that hUCB-MSC CM is pro-osteogenic, anti-osteoclastogenic, and also enhances osteocyte survival and function, thereby rendering all parameters of the bone microenvironment in favor of maintaining and increasing bone mass.

We believe that our results provide the first evidence suggesting the possibility of using hUCB-MSCs in the treatment or prevention of osteoporosis. Given the relative ease of procurement of hUCB-MSCs and better immune tolerance of hUCB-MSCs, our results clearly shed light on the use of stem cell therapy in the field of metabolic bone diseases.

Acknowledgments

This study was supported by a grant (No. A100675) from the Ministry of Health and Welfare of Korea and a grant (No. 2009-0077579) from the Ministry of Education, Science, and Technology of Korea.

Disclosure Statement

No competing financial interests exist.

References

1. Burge, R., Dawson-Hughes, B., Solomon, D.H., Wong, J.B., King, A., and Tosteson, A. Incidence and economic burden of osteoporosis-related fractures in the United States, 2005–2025. J Bone Miner Res **22,** 465, 2007.
2. Body, J.J., Bergmann, P., Boonen, S., Boutsen, Y., Devogelaer, J.P., Goemaere, S., *et al.* Evidence-based guidelines for the pharmacological treatment of postmenopausal osteoporosis: a consensus document by the Belgian Bone Club. Osteoporos Int **21,** 1657, 2010.
3. Schilcher, J., Michaelsson, K., and Aspenberg, P. Bisphosphonate use and atypical fractures of the femoral shaft. N Engl J Med **364,** 1728, 2011.
4. Ruggiero, S.L. Bisphosphonate-related osteonecrosis of the jaw: an overview. Ann N Y Acad Sci **1218,** 38, 2011.
5. Orwoll, E.S., Scheele, W.H., Paul, S., Adami, S., Syversen, U., Diez-Perez, A., *et al.* The effect of teriparatide [human parathyroid hormone (1–34)] therapy on bone density in men with osteoporosis. J Bone Miner Res **18,** 9, 2003.
6. Miyauchi, A., Matsumoto, T., Shigeta, H., Tsujimoto, M., Thiebaud, D., and Nakamura, T. Effect of teriparatide on bone mineral density and biochemical markers in Japanese women with postmenopausal osteoporosis: a 6-month dose-response study. J Bone Miner Metab **26,** 624, 2008.
7. Florenzano, F., and Minguell, J.J. Autologous mesenchymal stem cell transplantation after acute myocardial infarction. Am J Cardiol **95,** 435, 2005.
8. Imanishi, Y., Saito, A., Komoda, H., Kitagawa-Sakakida, S., Miyagawa, S., Kondoh, H., *et al.* Allogenic mesenchymal stem cell transplantation has a therapeutic effect in acute myocardial infarction in rats. J Mol Cell Cardiol **44,** 662, 2008.
9. Jeong, S.W., Chu, K., Jung, K.H., Kim, S.U., Kim, M., and Roh, J.K. Human neural stem cell transplantation promotes functional recovery in rats with experimental intracerebral hemorrhage. Stroke **34,** 2258, 2003.
10. Lee, H.J., Kim, K.S., Kim, E.J., Choi, H.B., Lee, K.H., Park, I.H., *et al.* Brain transplantation of immortalized human

neural stem cells promotes functional recovery in mouse intracerebral hemorrhage stroke model. Stem Cells **25,** 1204, 2007.
11. Voltarelli, J.C., Couri, C.E., Stracieri, A.B., Oliveira, M.C., Moraes, D.A., Pieroni, F., *et al.* Autologous nonmyeloablative hematopoietic stem cell transplantation in newly diagnosed type 1 diabetes mellitus. JAMA **297,** 1568, 2007.
12. Bhansali, A., Upreti, V., Khandelwal, N., Marwaha, N., Gupta, V., Sachdeva, N., *et al.* Efficacy of autologous bone marrow-derived stem cell transplantation in patients with type 2 diabetes mellitus. Stem Cells Dev **18,** 1407, 2009.
13. Mobasheri, A., Csaki, C., Clutterbuck, A.L., Rahmanzadeh, M., and Shakibaei, M. Mesenchymal stem cells in connective tissue engineering and regenerative medicine: applications in cartilage repair and osteoarthritis therapy. Histol Histopathol **24,** 347, 2009.
14. Kumar, S., Wan, C., Ramaswamy, G., Clemens, T.L., and Ponnazhagan, S. Mesenchymal stem cells expressing osteogenic and angiogenic factors synergistically enhance bone formation in a mouse model of segmental bone defect. Mol Ther **18,** 1026, 2010.
15. Zhao, M., Zhou, J., Li, X., Fang, T., Dai, W., Yin, W., *et al.* Repair of bone defect with vascularized tissue engineered bone graft seeded with mesenchymal stem cells in rabbits. Microsurgery **31,** 130, 2011.
16. Kim, D., Cho, S.W., Her, S.J., Yang, J.Y., Kim, S.W., Kim, S.Y., *et al.* Retrovirus-mediated gene transfer of receptor activator of nuclear factor-kappaB-Fc prevents bone loss in ovariectomized mice. Stem Cells **24,** 1798, 2006.
17. Cho, S.W., Sun, H.J., Yang, J.Y., Jung, J.Y., An, J.H., Cho, H.Y., *et al.* Transplantation of mesenchymal stem cells overexpressing RANK-Fc or CXCR4 prevents bone loss in ovariectomized mice. Mol Ther **17,** 1979, 2009.
18. Timmers, L., Lim, S.K., Arslan, F., Armstrong, J.S., Hoefer, I.E., Doevendans, P.A., *et al.* Reduction of myocardial infarct size by human mesenchymal stem cell conditioned medium. Stem Cell Res **1,** 129, 2007.
19. Timmers, L., Lim, S.K., Hoefer, I.E., Arslan, F., Lai, R.C., van Oorschot, A.A., *et al.* Human mesenchymal stem cell-conditioned medium improves cardiac function following myocardial infarction. Stem Cell Res **6,** 206, 2011.
20. Chen, L., Tredget, E.E., Wu, P.Y., and Wu, Y. Paracrine factors of mesenchymal stem cells recruit macrophages and endothelial lineage cells and enhance wound healing. PLoS One **3,** e1886, 2008.
21. Walter, M.N., Wright, K.T., Fuller, H.R., MacNeil, S., and Johnson, W.E. Mesenchymal stem cell-conditioned medium accelerates skin wound healing: an *in vitro* study of fibroblast and keratinocyte scratch assays. Exp Cell Res **316,** 1271, 2010.
22. Lim, H.C., Lee, S.T., Chu, K., Joo, K.M., Kang, L., Im, W.S., *et al.* Neuroprotective effect of neural stem cell-conditioned media in *in vitro* model of Huntington's disease. Neurosci Lett **435,** 175, 2008.
23. Mendes, S.C., Tibbe, J.M., Veenhof, M., Bakker, K., Both, S., Platenburg, P.P., *et al.* Bone tissue-engineered implants using human bone marrow stromal cells: effect of culture conditions and donor age. Tissue Eng **8,** 911, 2002.
24. Stenderup, K., Justesen, J., Clausen, C., and Kassem, M. Aging is associated with decreased maximal life span and accelerated senescence of bone marrow stromal cells. Bone **33,** 919, 2003.
25. Stolzing, A., Jones, E., McGonagle, D., and Scutt, A. Age-related changes in human bone marrow-derived mesenchymal stem cells: consequences for cell therapies. Mech Ageing Dev **129,** 163, 2008.
26. Tisato, V., Naresh, K., Girdlestone, J., Navarrete, C., and Dazzi, F. Mesenchymal stem cells of cord blood origin are effective at preventing but not treating graft-versus-host disease. Leukemia **21,** 1992, 2007.
27. Majhail, N.S., Brunstein, C.G., Tomblyn, M., Thomas, A.J., Miller, J.S., Arora, M., *et al.* Reduced-intensity allogeneic transplant in patients older than 55 years: unrelated umbilical cord blood is safe and effective for patients without a matched related donor. Biol Blood Marrow Transplant **14,** 282, 2008.
28. Rebelatto, C.K., Aguiar, A.M., Moretao, M.P., Senegaglia, A.C., Hansen, P., Barchiki, F., *et al.* Dissimilar differentiation of mesenchymal stem cells from bone marrow, umbilical cord blood, and adipose tissue. Exp Biol Med (Maywood) **233,** 901, 2008.
29. Guillot, P.V., De Bari, C., Dell'Accio, F., Kurata, H., Polak, J., and Fisk, N.M. Comparative osteogenic transcription profiling of various fetal and adult mesenchymal stem cell sources. Differentiation **76,** 946, 2008.
30. Yang, S.E., Ha, C.W., Jung, M., Jin, H.J., Lee, M., Song, H., *et al.* Mesenchymal stem/progenitor cells developed in cultures from UC blood. Cytotherapy **6,** 476, 2004.
31. Liu, Y., Ding, Y., Ma, P., Wu, Z., Duan, H., Liu, Z., *et al.* Enhancement of long-term proliferative capacity of rabbit corneal epithelial cells by embryonic stem cell conditioned medium. Tissue Eng Part C Methods **16,** 793, 2010.
32. Yoo, J.J., Song, W.S., Koo, K.H., Yoon, K.S., and Kim, H.J. Osteogenic abilities of bone marrow stromal cells are not defective in patients with osteonecrosis. Int Orthop **33,** 867, 2009.
33. Pittenger, M.F., Mackay, A.M., Beck, S.C., Jaiswal, R.K., Douglas, R., Mosca, J.D., *et al.* Multilineage potential of adult human mesenchymal stem cells. Science **284,** 143, 1999.
34. Bellino, F.L. Nonprimate animal models of menopause: workshop report. Menopause **7,** 14, 2000.
35. Erben, R.G. Embedding of bone samples in methylmethacrylate: an improved method suitable for bone histomorphometry, histochemistry, and immunohistochemistry. J Histochem Cytochem **45,** 307, 1997.
36. Becker, H.M., Chen, M., Hay, J.B., and Cybulsky, M.I. Tracking of leukocyte recruitment into tissues of mice by *in situ* labeling of blood cells with the fluorescent dye CFDA SE. J Immunol Methods **286,** 69, 2004.
37. Chou, M.Y., Yan, D., Jafarov, T., and Everett, E.T. Modulation of murine bone marrow-derived CFU-F and CFU-OB by *in vivo* bisphosphonate and fluoride treatments. Orthodont Craniofac Res **12,** 141, 2009.
38. An, J.H., Yang, J.Y., Ahn, B.Y., Cho, S.W., Jung, J.Y., Cho, H.Y., *et al.* Enhanced mitochondrial biogenesis contributes to Wnt induced osteoblastic differentiation of C3H10T1/2 cells. Bone **47,** 140, 2010.
39. Cho, S.W., Yang, J.Y., Her, S.J., Choi, H.J., Jung, J.Y., Sun, H.J., *et al.* Osteoblast-targeted overexpression of PPARgamma inhibited bone mass gain in male mice and accelerated ovariectomy-induced bone loss in female mice. J Bone Miner Res **26,** 1939, 2011.
40. Oh, W., Kim, D.S., Yang, Y.S., and Lee, J.K. Immunological properties of umbilical cord blood-derived mesenchymal stromal cells. Cell Immunol **251,** 116, 2008.

41. Cho, S.W., Sun, H.J., Yang, J.Y., Jung, J.Y., Choi, H.J., An, J.H., *et al.* Human adipose tissue-derived stromal cell therapy prevents bone loss in ovariectomized nude mouse. Tissue Eng Part A **18,** 1067, 2012.
42. Nakanishi, C., Yamagishi, M., Yamahara, K., Hagino, I., Mori, H., Sawa, Y., *et al.* Activation of cardiac progenitor cells through paracrine effects of mesenchymal stem cells. Biochem Biophys Res Commun **374,** 11, 2008.
43. Jung, J., Moon, N., Ahn, J.Y., Oh, E.J., Kim, M., Cho, C.S., *et al.* Mesenchymal stromal cells expanded in human allogenic cord blood serum display higher self-renewal and enhanced osteogenic potential. Stem Cells Dev **18,** 559, 2009.
44. Bonewald, L.F. The amazing osteocyte. J Bone Miner Res **26,** 229, 2011.
45. Barragan-Adjemian, C., Nicolella, D., Dusevich, V., Dallas, M.R., Eick, J.D., and Bonewald, L.F. Mechanism by which MLO-A5 late osteoblasts/early osteocytes mineralize in culture: similarities with mineralization of lamellar bone. Calcif Tissue Int **79,** 340, 2006.
46. Dunstan, C.R., Evans, R.A., Hills, E., Wong, S.Y., and Higgs, R.J. Bone death in hip fracture in the elderly. Calcif Tissue Int **47,** 270, 1990.
47. Wong, S.Y., Evans, R.A., Needs, C., Dunstan, C.R., Hills, E., and Garvan, J. The pathogenesis of osteoarthritis of the hip. Evidence for primary osteocyte death. Clin Orthop Relat Res **214,** 305, 1987.
48. Weinstein, R.S., Nicholas, R.W., and Manolagas, S.C. Apoptosis of osteocytes in glucocorticoid-induced osteonecrosis of the hip. J Clin Endocrinol Metab **85,** 2907, 2000.

Address correspondence to:
Chan Soo Shin, MD, PhD
Department of Internal Medicine
Seoul National University College of Medicine
28 Yungun-Dong, Chongno-Gu
Seoul 110-744
Korea

E-mail: csshin@snu.ac.kr

Received: January 27, 2012
Accepted: September 21, 2012
Online Publication Date: January 4, 2013